AIAA Guidance, Navigation, and Control Conference
2 - 5 August 2010, Toronto, Ontario Canada

AIAA 2010-7512

Longitudinal Stability Analysis of a Jet-Powered Wingsuit

Geoffrey Robson* and Raffaello D'Andrea*

Over the past decade wingsuits have gone from being the preserve of stuntmen to being readily accessible to sufficiently experienced skydivers. They are now a familiar sight at drop zones, but have so far not been the subject of academic study. In this paper we use well known aerodynamic laws to propose a glide equation for wingsuits, and use accurate flight data both to validate the equation and to infer the two parameters that appear in it. Powered flight is then considered, and the thrust required for sustained level flight is calculated. We then describe a model for the longitudinal stability of wingsuit flight and show that with the thrust configuration used by Visa Parviainen (small gas turbine engines secured to his feet), phugoid mode instability is the likely explanation for the uncontrollable speed changes he has experienced, and propose automatic thrust vectoring as a means of preventing these.

I. Introduction

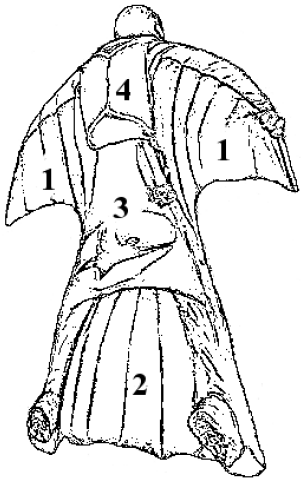

Figure 1. The Vampire 3 wingsuit in full flight. The numbered components are the (1) arm-wings, (2) leg-wing, (3) deflector, and (4) parachute.

A wingsuit may be defined as a wearable suit constructed from an appropriate fabric that is flexible, intimately connected to the body, and designed to maximise the wearer's freefall time or glide ratio. A clear distinction must be made between wingsuits and the rigid wings used by Yves Rossy,[11] or proposed designs[8] that even include an open fuselage. While these may have performance advantages over wingsuits and be of interest for military applications,[2] their rigid structures compromise the intimacy of the flight experience, with the user being more a pilot than a flyer. In contrast, a wingsuit offers humans the opportunity to experience flight in much the same way a bird must.

For a non-technical account of wingsuit history, the interested reader is referred to Abrams.[1] Much of this history, which dates back to the 1930s, involved daredevils and stuntmen who constructed their own experimental wingsuits, with mixed – and sometimes fatal – results. But in the last decade the combination of mature wingsuit design and modern, highly reliable parachutes, has enabled anyone with a reasonable degree of physical fitness, balance, and courage, to learn to fly them.

The basic principle of a wingsuit is to generate lift with webbing spread between each arm and the body, and between the legs. To do so efficiently requires an airfoil profile, and in all modern wingsuits (like the Vampire 3 from Phoenix-Fly[a] shown in Fig. 1) this is achieved using the same double-skinned, cellular, ram air design used for modern skydiving parachutes and paragliders. The result of this lift is a glide ratio of over 2:1, and a doubling of typical skydive freefall time from about 1 to 2 minutes.

*Institute for Dynamic Systems and Control, ETH Zürich, 8092 Zürich, Switzerland.
[a]http://www.phoenix-fly.com

II. The wingsuit glide equation

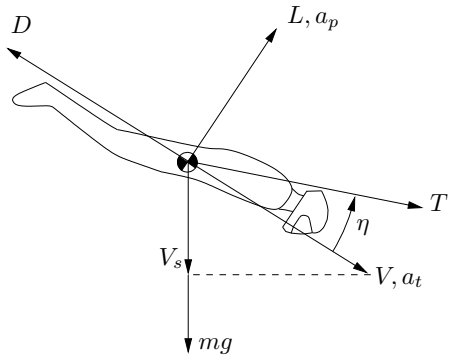

Figure 2. Force, acceleration, and velocity vectors of longitudinal wingsuit flight.

As with all heavier-than-air aircraft, a wingsuit's flight may be studied by considering the forces of lift L, drag D, weight mg, and thrust T acting on it. Fig. 2 shows these forces and the resulting accelerations and velocities. Thrust is included for use in later sections. We consider only longitudinal flight, so two equations of motion are required. That along the flight path is

$$mg\frac{V_s}{V} - D + T\cos\eta = ma_t, \tag{1}$$

where V is the speed, V_s the downward (sinking) component of the speed, and a_t the acceleration tangential to the flight path. In the direction perpendicular to the flight path, the equation of motion is

$$L - mg\sqrt{1 - \left(\frac{V_s}{V}\right)^2} + T\sin\eta = ma_p, \tag{2}$$

where a_p is the acceleration perpendicular to the flight path.

We follow the approach taken by Tucker[15] in his study of gliding birds by splitting the drag into induced and parasitic components. He makes the further distinction of profile drag, but this is described mathematically in the same way as parasitic drag, so we have combined the two and refer to them jointly as parasitic drag. Implicit in the development below is the assumption that the wingsuit can be treated as one lifting surface. We will have to revisit this assumption when we consider longitudinal stability in Section V.

Induced drag is that produced as a direct result of lift generation, and may be modelled by

$$D_i = \frac{L^2}{c_i \rho V^2}, \tag{3}$$

where ρ is air density, and c_i a constant[b] proportional to the area of the lifting surface with units of m^2. Parasitic drag accounts for all other drag acting on the wingsuit, and may be modelled by

$$D_p = c_p \rho V^2, \tag{4}$$

where the constant c_p also has units of m^2, and is essentially the product of the cross-sectional area, the parasitic drag coefficient, and a factor of $\frac{1}{2}$, combined into one variable for brevity[c].

If (2) is solved for L, the result substituted into (3), and $D_i + D_p$ substituted for D in (1), then an equation that describes non-equilibrium flight is obtained. For the case of equilibrium gliding, the accelerations and thrust are zero, and the equation may then be solved for the sinking speed:

$$V_s = \frac{V}{g}\left(\sqrt{A(A+2B)+g^2} - A\right), \tag{5}$$

where

$$A := \frac{c_i \rho V^2}{2m}, \quad B := \frac{c_p \rho V^2}{m}. \tag{6}$$

The assumption made by Tucker[15] in deriving his expression for V_s is that the glide angle is small, and that its cosine may therefore be considered equal to one, which implies that lift equals weight. This is reasonable for the shallow and efficient glide of a bird, but the glide angle of a wingsuit is typically more than 20°, so the more complex expression in (5) is necessary.

The equilibrium glide ratio – the ratio of horizontal velocity to vertical velocity – may be calculated as

$$\sqrt{\left(\frac{V}{V_s}\right)^2 - 1}, \tag{7}$$

[b]The assumption being made is that the Reynolds number is sufficiently high (and its variation sufficiently low) that c_i (and c_p) may be considered constant.

[c]The same is done with the lift and drag factors defined later in this section.

which in combination with (5) allows it to be calculated as a function of speed, with the maximum glide ratio occurring when the speed is equal to

$$\sqrt{\frac{mg}{\rho\sqrt{c_p\left(c_i+4c_p\right)}}}. \tag{8}$$

It can also be shown that the equilibrium glide ratio is a monotonic increasing function of c_i, and a monotonic decreasing function of c_p, which is an intuitive result.

More subtle is Tucker's[15] explanation of why birds vary their wingspan at different gliding speeds. A reduction in wingspan reduces both c_p and c_i, and he shows that this can sometimes produce a better glide ratio than a fully extended wing. It may be possible to perform a similar optimization for wingsuit flight, although the relationship between c_p and c_i is not likely to be a simple function of body position.

The best way to determine accurately the values of c_i and c_p would be to perform wind tunnel tests on a wingsuit. A wind tunnel capable of tilting through the range of glide angles a wingsuit flies at would be ideal, and smaller versions of such a system have been used successfully for studying gliding birds.[10] The high airspeeds, large wind tunnel cross section, and large glide angles of wingsuit flight, however, make the development of such a tunnel unlikely. A conventional wind tunnel could instead be used, but this would require the careful development of a support for the wingsuit flyer, since equilibrium flight would not be possible.

Another approach, and the one taken in this paper, is to infer the parameters from wingsuit flight data. If the same steps in deriving (5) are taken, but the acceleration variables retained, the following non-equilibrium glide equation is obtained:

$$c_D = \frac{c_L^2}{c_i} + c_p, \tag{9}$$

where c_D is the drag factor, defined as

$$c_D := \frac{D}{\rho V^2} = \frac{m\left(g\frac{V_s}{V} - a_t\right)}{\rho V^2}, \tag{10}$$

and c_L the lift factor, defined as

$$c_L := \frac{L}{\rho V^2} = \frac{m\left(a_p + g\sqrt{1-\left(\frac{V_s}{V}\right)^2}\right)}{\rho V^2}. \tag{11}$$

If acceleration, velocity, and air density data are captured during a wingsuit flight, then values for c_L^2 and c_D may be plotted against each other, and if (9) is valid and the data sufficiently accurate, a linear relationship will be observed. Linear regression on these data could then be used to estimate the values of c_i and c_p.

III. Flight data measurements and analysis

The development of small MEMS-based inertial sensors has enabled their use in such wearable applications as the study of the aerodynamic forces on ski jumpers.[7] We chose the MTi-G from Xsens Technologies[d] for measuring flight data since, in addition to linear accelerometers and rate gyros, it also contains magnetometers, an integrated GPS and barometer, and a DSP for processing and fusing the data from all of these sensors in real time. Estimates of position, speed, acceleration, and orientation were streamed from the MTi-G over a serial link to a portable data logging device we constructed, which recorded these data to a MicroSD card.

The MTi-G was secured to the chest of the flyer[e] over the base of the sternum, and the GPS antenna to the back of his helmet to ensure optimal reception. Data were captured at 100 Hz, and the acceleration and rate gyro data low-pass filtered with a cut-off frequency of 2 Hz to mitigate the effects of vibration. It was also necessary to compensate for the distance of the MTi-G from the centre of gravity, which entailed estimation of angular acceleration from the filtered rate gyro data. We used the Vampire 3 wingsuit (see Fig. 1), which was designed for optimal glide ratio and introduced in October 2008.

[d] `http://www.xsens.com`
[e] The first author.

Data captured during a 4.1 second period were chosen for analysis. The period begins about 4.3 seconds after jumping, which is enough time for the ram air wings to inflate and body position to stabilise, but still well within the subterminal portion of the flight. This results in data with non-zero accelerations and a range of speeds and glide ratios, which provide for an excellent test of the validity of (9). A wide range of c_L^2 and c_D values were also produced, making the linear relationship predicted by (9) most obvious, and allowing for accurate estimates of c_i and c_p to be made.

Values of $c_i = 1.67$ and $c_p = 0.056$ were obtained from regression of these data, with the solid line in Fig. 3 showing how well the resulting linear relationship fits them. Using the formulae in[15] to calculate these parameters from first principles shows that for the dimensions of the wingsuit used, the values we inferred from our flight data are entirely plausible.

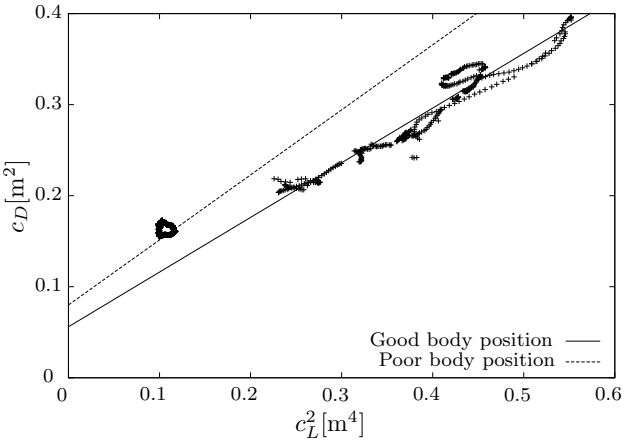

Figure 3. Subterminal and terminal flight data used for estimating c_i and c_p.

The small circular cluster of data in Fig. 3 at around $c_L^2 = 0.1$ was obtained from a 16 second period from the latter part of the same flight. Flight during this period was terminal and stable (i.e. in equilibrium), and the small accelerations recorded were likely due only to sensor vibration, and have thus been ignored to reduce the spread of c_L^2 and c_D values. A headwind of 2 m/s was also compensated for during this period[f]. After nearly a minute of flying, the altered body position resulting from fatigue has caused the data to deviate noticeably from the solid line. The values of c_i and c_p have changed during the flight, but performing linear regression on the small cluster of data would clearly be futile, so some other means of decoupling the parameters is needed. We used a combination of aerodynamic reasoning and flight experience to ascertain what the equilibrium glide curve should look like, and to infer how the values of c_i and c_p might be affected by shoulder fatigue (which results in the arms being swept upward and backward). Values of $c_i = 1.4$ and $c_p = 0.08$ were selected. The dashed line in Fig. 3 shows the resulting theoretical linear relationship for this poor body position.

Using a mass[g] of 83 kg and an air density[h] of 1 kg/m^3, we plot in Fig. 4 the equilibrium glide ratio for the poor and good body positions as a function of speed. Flying at around 35 m/s with one's arms swept back is comfortable and requires little concentration, but the plots are consistent with our experience of flying wingsuits in showing how important it is to maintain speed and good body position when attempting to fly as far as possible. Using the expression in (8) shows that the maximum glide ratio occurs at about 50 m/s for the good body position, although we must point out that flying that fast is not easy, so the more realistic speed of 45 m/s is used for calculations in the sections to follow.

A study of the relationship between lift and angle of attack α is made possible by the orientation data output by the MTi-G. It sits on the chest at a forward inclination estimated at 10° by standing in a neutral upright position (this offset was added to the raw data, so the datum for α is the coronal plane, represented in Fig. 7 by the dash-dot line).

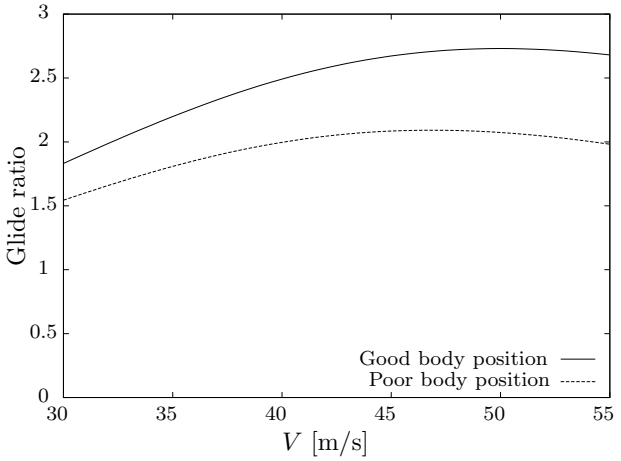

Figure 4. Equilibrium glide ratio as a function of speed for good and poor body positions.

[f]The values of c_L^2 and c_D are very sensitive to errors in V, so this correction – though small – is important.

[g]The mass of the flyer with gear.

[h]The value of $\rho = 1$ is convenient, but also representative of air density at the altitudes wingsuits are typically flown at.

We used the same subterminal data used to estimate c_i and c_p to produce the plot in Fig. 5 showing lift factor against angle of attack. The linear relationship predicted by aerodynamic theory[3] is observed, with linear regression yielding

$$c_L = 1.17\alpha + 0.39. \tag{12}$$

This function will be used extensively in later sections. Note that α (in common with all angles in this paper) is measured in radians, but displayed in figures and referenced in the text in degrees for ease of interpretation.

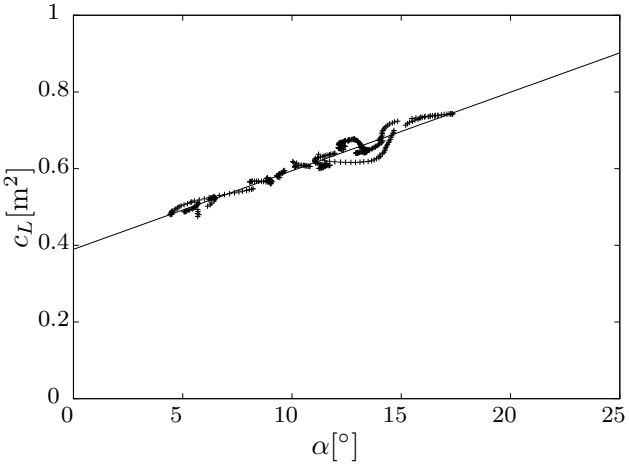

Figure 5. Subterminal flight data showing the linear relationship between c_L and angle of attack.

IV. Thrust requirements for level flight

In October 2005 Visa Parviainen became the first person to fly a powered wingsuit when he jumped from a hot air balloon near Lahti in Finland with two small gas turbine engines[i] secured to each of his feet. Very little altitude was lost during the 30 second period of powered flight.[9] We now consider the minimum thrust required for sustained level flight although, since a real propulsion system will have mass and increase parasitic drag, the results presented should be considered theoretical lower bounds.

The role of thrust in aviation is traditionally viewed as overcoming drag, but it can be beneficial to use some component of it to provide additional lift. This is especially true of aircraft like jet fighters with their low L/D ratios, and particularly relevant for those of the newer generation with thrust vectoring capabilities, since optimization of thrust angle for different flight regimes is possible.[4]

We apply the thrust at an upward angle η from the flight path (see Fig. 2 and Fig. 7), and determine the optimal value of this angle for level flight. In practice non-vectored thrust would be applied at a constant angle χ relative to the body, so η would be a function of the angle of attack:

$$\eta = \alpha + \chi, \tag{13}$$

as may be seen in Fig. 7. In conjunction with (12), we can therefore calculate the optimal thrust-body angle χ as a function of speed.

Repeating the steps taken in deriving (5), but this time retaining T and instead setting V_s to zero, yields

$$T = \frac{m}{\sin(\eta)}\left(C - \sqrt{C^2 - g^2 - 2AB}\right), \tag{14}$$

where A and B are defined as before, and

$$C := A\cot(\eta) + g. \tag{15}$$

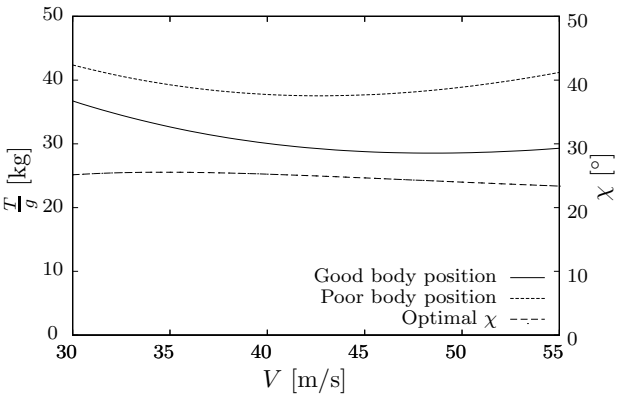

Figure 6. Minimum thrust required for level flight, and optimal χ for level flight in the good body position.

A closed-form expression for optimal η does not exist, but it and the corresponding minimum thrust are easily found with numerical techniques. This was done for a range of speeds, with Fig. 6 showing that the minimum thrust varies only somewhat with speed, but increases significantly as body position deteriorates. Also plotted is optimal χ, which is seen to be almost independent of speed[j]. This is clearly convenient from a design standpoint, since a fixed angle of perhaps 25° could be used, resulting in about an 8% reduction in thrust required had χ simply been set to zero.

[i] Artes Jet JF-160 Rhinos, each capable of 16 kg of thrust.

[j] This is for the good body position, since (12) was derived only from the subterminal data.

V. Longitudinal stability analysis

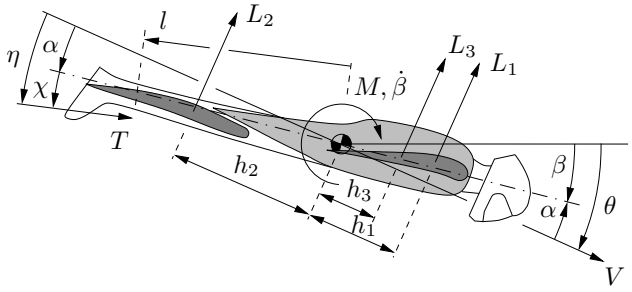

Figure 7. Cross section of the Vampire 3 wingsuit.

We begin our analysis by rewriting (1) and (2) in terms of state variables speed V, glide angle θ, body pitch angle β, and body pitch angle rate $\dot{\beta}$. The two translational equations of motion are then

$$\dot{V} = \frac{T\cos\eta - D}{m} + g\sin\theta \tag{16}$$

and

$$\dot{\theta} = \frac{1}{V}\left(g\cos\theta - \frac{L + T\sin\eta}{m}\right), \tag{17}$$

with the rotational equation of motion being

$$\ddot{\beta} = \frac{M}{I}, \tag{18}$$

where M is the nose-down pitching moment about the centre of gravity, and I the moment of inertia of the body. The centre of gravity and I were estimated,[12] with I set to 16 kg $\cdot$ m^2.

In order to characterize the pitching moment, the total lift is assumed to be produced by the three main lifting surfaces, identified in Fig. 1 as the arms-wings, the leg-wing, and the combination of the torso and deflector. These are shown in cross section in Fig. 7, along with their moment arms h_k of 0.30, 0.65, and 0.20 m, respectively. The lift generated by each surface is assumed to be of the form

$$L_k = \rho V^2 c_{L_k}, \quad c_{L_k} = s_k\alpha_k + q_k \tag{19}$$

where α_k is the *local* angle of attack seen by lifting surface k; using the notation in Fig. 7, these are approximated by

$$\alpha_1 = \alpha - \frac{h_1\dot{\alpha}}{V}, \;\; \alpha_2 = \alpha + \frac{h_2\dot{\alpha}}{V}, \;\; \alpha_3 = \alpha - \frac{h_3\dot{\alpha}}{V}. \tag{20}$$

The sum of the three s_k – the partial derivatives of the lift factors with respect to α – must equal the total for the wingsuit, which from (12) is seen to be 1.17 m^2/rad. Subject to this constraint, the s_k were estimated to be 0.41, 0.56, and 0.20 m^2/rad, respectively, with a Java applet called FoilSim II on NASA's website[k] used to arrive at these values. Using the dimensions of the wingsuit's lifting surfaces and estimates of camber based on observations of the wingsuit in flight, FoilSim II was found to produce results pleasingly consistent with our experimental observations.

We assume that the pitching moment is dominated by the lift produced by the three lifting surfaces:

$$M = \rho V^2\left(c_m\alpha + \frac{c_{md}}{V}\dot{\alpha} + (-h_1q_1 + h_2q_2 - h_3q_3)\right), \tag{21}$$

where

$$c_m := -s_1h_1 + s_2h_2 - s_3h_3 = 0.20 \text{ m}^3/\text{rad}, \quad c_{md} := s_1h_1^2 + s_2h_2^2 + s_3h_3^2 = 0.28 \text{ m}^4/\text{rad}. \tag{22}$$

It should be noted, however, that even though the contribution of drag forces to pitching moment are usually negligible in aircraft[3] and birds,[6] the low L/D ratio of a wingsuit makes this assumption questionable. Some flying animals are even believed to rely on drag-based stability,[14] of which the flying squirrel is an especially relevant example[l]. The values for c_m and c_{md} derived above are thus likely underestimates. Fortunately, the subsequent analysis is quite insensitive to these values.

Also note that the pitching moment at equilibrium must be zero, which implies that the derivative of M with respect to the state variable V is therefore also zero. This fact will be used in the subsequent stability analysis.

The rate of change of the angle of attack has a substantial impact on the rotational dynamics via the damping term $(c_{md}/V)\dot{\alpha}$, which was derived by decomposing the total lift into three lifting surfaces. It

[k] `http://www.grc.nasa.gov/WWW/K-12/FoilSim/`

[l] Less relevant is its means of drag-based stability – a long furry tail!

can be shown, however, that it has a negligible impact on the translational dynamics, and we thus use the previously derived expressions for the total lift and drag:

$$L = \rho V^2 c_L \tag{23}$$

and

$$D = \rho V^2 c_D = \rho V^2 \left(c_p + \frac{c_L^2}{c_i} \right), \tag{24}$$

where c_L is the linear function of α defined in (12). In particular, we treat the wingsuit as one lifting surface when considering the translational dynamics.

We see in Fig. 7 that α is itself simply equal to $\theta - \beta$, which also allows the thrust angle to be written as

$$\eta = \theta - \beta + \chi, \tag{25}$$

and since the thrust of an ideal jet may be considered independent of V (and of θ and β),[3] the derivatives of $\dot{V}$ and $\dot{\theta}$ with respect to the state variables are easily obtained.

Rigid body dynamics have until now been implicitly assumed, but a real system would have numerous imperfections that could cause the thrust not to act through the centre of gravity. It is reasonable to suppose that the resulting moment could have a destabilising effect, so it is important that some form of non-rigidity be modelled.

One way of achieving this is to assume that the thrusters are mounted to the body through a frictionless bearing, so that no turning moment can be applied to them. The thrust angle η would then be unaffected by changes in the body pitch angle β. This is probably an overly pessimistic assumption, so we propose instead that thrust angle be modelled as

$$\eta = \theta - (\beta_0 + r(\beta - \beta_0)) + \chi, \tag{26}$$

where β_0 is the equilibrium body pitch angle and r a *rigidity factor* between zero and one. When it is one, (26) is identical to (25), and a perfect rigid body is modelled. When zero, the frictionless bearing scenario is modelled, so varying r allows for the likely effects of non-rigidity to be studied without the need for an elaborate extension to the system model or the introduction of new state variables. The moment produced by a small change in body pitch angle may then be shown to be

$$Tl(1 - r)(\beta - \beta_0), \tag{27}$$

where l is the position of the thrusters relative to the centre of gravity, assumed to be 1 m.

We are now in a position to linearise the state space equations about an equilibrium point and derive the system state matrix equation:

$$\begin{bmatrix} \ddot{\beta} \\ \dot{\beta} \\ \dot{V} \\ \dot{\theta} \end{bmatrix} = \begin{bmatrix} a_1 & a_2 & 0 & a_3 \\ 1 & 0 & 0 & 0 \\ 0 & a_4 & a_5 & a_6 \\ 0 & a_7 & a_8 & a_9 \end{bmatrix} \begin{bmatrix} \dot{\beta} \\ \Delta\beta \\ \Delta V \\ \Delta\theta \end{bmatrix} + \begin{bmatrix} 0 \\ 0 \\ b_1 \\ b_2 \end{bmatrix} \Delta T, \tag{28}$$

where Δ denotes deviation of a particular state variable about its equilibrium value, and ΔT is the only control input considered. The eleven partial derivatives in the system and input matrices may be shown to be:

$$a_1 := \frac{\partial \ddot{\beta}}{\partial \dot{\beta}} = \frac{-c_{md}\rho V}{I}$$

$$a_2 := \frac{\partial \ddot{\beta}}{\partial \beta} = \frac{1}{I}(Tl(1 - r) - c_m \rho V^2)$$

$$a_3 := \frac{\partial \ddot{\beta}}{\partial \theta} = \frac{c_m \rho V^2}{I}$$

$$a_4 := \frac{\partial \dot{V}}{\partial \beta} = \frac{2\rho V^2 c_L}{m c_i} \frac{\partial c_L}{\partial \alpha} + \frac{rT \sin \eta}{m}$$

$$
\begin{aligned}
a_5 &:= \frac{\partial \dot{V}}{\partial V} = \frac{-2\rho V c_D}{m} \\
a_6 &:= \frac{\partial \dot{V}}{\partial \theta} = \frac{\rho V^2 c_L}{m}\left(1 - \frac{2}{c_i}\frac{\partial c_L}{\partial \alpha}\right) \\
a_7 &:= \frac{\partial \dot{\theta}}{\partial \beta} = \frac{\rho V}{m}\frac{\partial c_L}{\partial \alpha} + \frac{rT\cos\eta}{mV} \\
a_8 &:= \frac{\partial \dot{\theta}}{\partial V} = \frac{-2\rho c_L}{m} \\
a_9 &:= \frac{\partial \dot{\theta}}{\partial \theta} = \frac{-\rho V}{m}\left(c_D + \frac{\partial c_L}{\partial \alpha}\right) \\
b_1 &:= \frac{\partial \dot{V}}{\partial T} = \frac{\cos\eta}{m} \\
b_2 &:= \frac{\partial \dot{\theta}}{\partial T} = -\frac{\sin\eta}{mV}.
\end{aligned}
\tag{29}
$$

Calculating these for gliding flight at a speed of 45 m/s and determining the eigenvalues and eigenvectors of the system matrix reveals two well-known stable oscillatory modes.

The first is the phugoid mode, in which angle of attack remains roughly constant and speed and glide angle oscillate slowly with a period of about 22 seconds, decaying with a time constant of about 9 seconds. The second is the short-period mode, in which speed and glide angle remain roughly constant, and the body pitches about its centre of gravity, with frequency of about 0.80 Hz and decaying with a time constant of about 1.4 seconds.

When powered level flight with $r = 1$ and $\chi = 25°$ is considered, the only significant change to these modes is a decrease in phugoid mode damping, with the time constant of oscillation decay increasing to about 15 seconds. But when r is reduced to 0.74 the phugoid mode becomes unstable, although the short-period mode changes little and remains stable even as r is reduced to zero. The influence of χ was found to be negligible.

It is not unreasonable to assume that a value of $r \approx 0.7$ could be representative of a real system's non-rigidity, but even if it were much higher, flight could still become very unsteady if the thrust input varied at a frequency close to that of the phugoid mode. With $r = 0.9$ and a thrust fluctuation of about 10%, significant speed resonance could result, as is seen in the frequency response plots of Fig. 8.

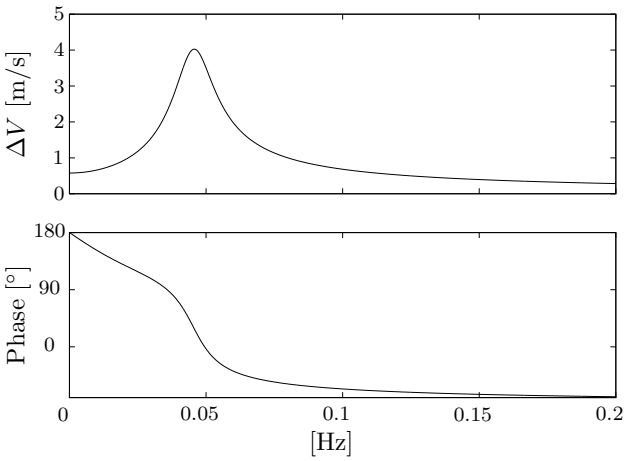

Figure 8. The effect on speed of a fluctuating control thrust of $\Delta T = 30$ N, with $r = 0.9$.

VI. Conclusions and further work

The thrust required for sustained level flight has been shown both in practice, and now in theory, to be entirely feasible. However, at least three problems limit the practical utility of powered wingsuits.

The first is the deterioration of body position due to fatigue, which greatly increases thrust requirements, and of course decreases the comfort of the flyer. A means of reducing the load on the shoulders without compromising the intimacy of the flying experience would be of great benefit to both powered and regular wingsuit flight.

The second is the vulnerability of the system to phugoid mode instability. Even when gliding, we know from practical experience that maintaining a constant speed is difficult and requires practice. A possible explanation for this is the difficulty the flyer has in gauging the system's state. Stationary objects are too far away to be useful as visual references, so the only senses that can be relied upon are the forces and accelerations felt, and to a lesser extent, the sound of the airflow. So despite the slow dynamics of the phugoid mode, humans are limited in their ability to control it because of the poor state information available to them. It may well be feasible for a fly-by-wire system to assist the flyer in controlling the phugoid mode dynamics. Despite the slow responsiveness of gas turbine engines, thrust control alone would probably be sufficient, but there are several reasons to favour thrust vectoring instead. Thrust is critical to performance, so one would want to be able to run the engines at or very near their full power for extended periods. Leaving enough capacity reserve to allow for thrust to be used as an effective control input would prevent this. Gas turbine engines are also best suited to applications that allow them to be run at a constant speed, so using thrust as a control input could very well have negative efficiency and even reliability implications. Thrust vectoring would avoid these problems, and also have the advantage of allowing for automatic compensation of engine misalignment and leg movements. Thrust vectoring systems on the radio-controlled model aircraft – for which the gas turbines used by Visa were designed – have begun to appear in recent years. Such a system (though admittedly for a ducted fan, not a pure jet) has been used successfully for damping the problematic phugoid mode on model aircraft,[5] and we believe it could also be used to stabilise powered wingsuit flight.

The third problem with powered (and unpowered) wingsuits is their inefficiency in lateral flight. Aggressive turns or barrel rolls cause immediate and considerable altitude loss, which in practice means that wingsuit flying is usually quite conservative, with lateral flight typically limited to slowly executed turns. Vectored thrust in the lateral plane could change this, but because the flyer's entire body is engaged in flying the wingsuit, it is not obvious how such vectoring could be controlled. An ambitious but compelling solution would be to measure body movements to determine the flyer's imminent flight manoeuvre, and then enhance this with thrust vectoring. An example of a system capable of measuring the necessary body movements is the MVN from Xsens Technologies, which uses 17 MEMS-based inertial trackers to map body position to a 23 segment model of the human skeleton. The combination of the MVN and MTi-G could also be used for the comprehensive study of the variation of such parameters as c_i and c_p with body position that would be required for the proposed human flight performance augmentation system to be feasible.

References

[1]Abrams, M. (2006), *Birdmen, Batmen, and Skyflyers*, Harmony Books, New York.

[2]Brasfield, S. (2008), *Innovations in Air Insertion (involving parachutes)*, Master's Thesis, Naval Postgraduate School, Monterey, California.

[3]Etkin, B., and Reid, L.D. (1996), *Dynamics of Flight*, Third Edition, John Wiley & Sons.

[4]Gilyard, G.B., and Bolonkin, A. (2000), Optimal pitch thrust-vector angle and benefits for all flight regimes, NASA-TM-2000-209021.

[5]Kannan, N. and Bhat, M.S. (2005), Longitudinal H_∞ stability augmentation system for a thrust-vectored unmanned aircraft, *Journal of Guidance, Control, and Dynamics*, **28**, No. 6, 1240–1250, American Inst. of Aeronautics and Astronautics.

[6]Krus, P. (1997), Natural methods for flight stability in birds, *AIAA and SAE, 1997 World Aviation Congress*.

[7]Ohgi, Y., Hirai, N., Murakami, M., and Seo, K. (2008), Aerodynamic study of ski jumping flight based on inertia sensors (171), *The Engineering of Sport 7*, **2**, 157–164, Springer.

[8]Johnson, K.T., Sullivan, M.R., Sutton, J.E., Mourtos, N.J. (2009), Design of a skydiving glider, *Proceedings, Aerospace Engineering Systems Workshop, WSEAS*.

[9]Parviainen, V. (2009), Personal communication.

[10]Rosén, M., and Hedenström, A. (2001), Gliding flight in a jackdaw: a wind tunnel study, *Journal of Experimental Biology*, **204**, 1153–1166.

[11]Rossy, Y. and To, F.E. (2002), Pneumatic gliding wing for a freefall jumper, US Patent App. 10/496,171.

[12]Santschi, W.R., and DuBois, J. and Omoto, C. (1963), Moments of inertia and centers of gravity of the living human body, Technical Documentary Report No. AMRL-TDR-63-36.

[13]Siciliano, B., and Khatib, O. (2008), *Springer Handbook of Robotics*, ISBN 354023957X, Springer.

[14]Thomas, A.L.R., and Taylor, G.K. (2001), Animal flight dynamics I. Stability in gliding flight, *Journal of Theoretical Biology*, **212**, 399–424, Elsevier.

[15]Tucker, V.A. (1987), Gliding birds: The effect of variable wing span, *Journal of Experimental Biology*, **133**, 33–58.